Review—Mitigating Supercapacitor Self-Discharge Through Strategic Materials Modification

Journal of The Electrochemical Society, 2021 **168** 090562
1945-7111/2021/168(9)/090562/12/$40.00 © 2021 The Electrochemical Society ("ECS"). Published on behalf of ECS by IOP Publishing Limited

Review—Mitigating Supercapacitor Self-Discharge Through Strategic Materials Modification

Ajay D. Jagadale,[1,z] R. C. Rohit,[1] Surendra K. Shinde,[2] and D.-Y. Kim[2]

[1]*Centre for Energy Storage and Conversion, School of Electrical and Electronics Engineering, SASTRA Deemed University, Thanjavur 613401, Tamil Nadu, India*
[2]*Department of Biological and Environmental Science, College of Life Science and Biotechnology, Dongguk University, Biomedical Campus, Ilsandong-gu, Siksa-dong, 10326, Goyang-si, Gyeonggi-do, Republic of Korea*

A high-power density, rapid charge-discharge and long cycle life are important features of supercapacitors (SCs). However, SCs are mainly suffered from their high self-discharge (SD) which is a spontaneous decay of voltage with time under open-circuit conditions. Due to SD behavior, SCs cannot be employed or coupled with many important energy harvesting devices including piezoelectric and triboelectric nanogenerators. It is highly desired to develop different innovative strategies to mitigate the SD. This review aims at discussing a SD mechanism and reviewing different mitigation strategies based on the modification of materials and devices. We discuss design, underlying principle, mechanism of the mitigation strategies and corresponding SD performance in detail. Moreover, the summary and prospects in this field have been provided. It is recommended to test an individual electrode for SD, identify the mechanism and develop different strategies for suppression. This review will be beneficial for researchers around the world to have a better understanding of the SD mechanism and to develop innovative strategies for SD mitigation and thereby the high-performance SCs.
 [DOI: 10.1149/1945-7111/ac275d]

Manuscript submitted May 21, 2021; revised manuscript received September 4, 2021. Published September 27, 2021.

As a high-performance energy storage device, supercapacitor (SC) has gained major interest owing to its rapid charging-discharging ability, high power density and long cycle life.[1–5] Based on electrode material used, SCs are classified into electric double-layer capacitors (EDLC) and pseudocapacitors.[6–9] The EDLC stores charge via physical adsorption/desorption of electrolytic ions on the electrode surface, whereas, pseudocapacitor stores charge via fast redox reaction at/near the surface of the electrode.[10–12] SCs are normally characterized by their energy density, power density and cycle life, however, one of the important parameters, such as self-discharge (SD) is often ignored by the research community.[13,14] The SD is nothing but the spontaneous voltage decay of charged SC with time in the absence of an external load. Since the energy and power densities are voltage-dependent parameters, the loss of a significant amount of energy due to SD has raised a question on the energy storage efficiency of SCs. The SD rate in SCs is greater than the batteries, in conventional SCs, the voltage reduces about 40% after 12 h.[15] This is a serious decrement since SCs are mainly utilized in the first half of their operating potential window. Owing to this limiting character, SCs cannot be employed or coupled with many important energy harvesting devices including piezoelectric and triboelectric nanogenerators.[16] Previously, different models have been developed to study and predict the SD mechanism.[17–20] The SD originates due to the higher thermodynamic state of the charged SCs from which it finds ways to naturally relax and return to the lower energy state (uncharged). In general, the main contributions to the SD are ohmic leakage, parasitic faradaic reaction and charge redistribution.[21–23] It is imperative to identify the main SD mechanism involved in a particular electrode or device and develop different strategies to mitigate it. Previously, different strategies have been developed and effectively employed on the materials and device level. However, in literature, most of the SD profiles are obtained for full cells rather than for individual electrodes. Besides, the data has been poorly analyzed and presented. Therefore, it is the need of the hour to discuss different SD mechanisms, find efficient methodologies for identifying the mechanism and recognize effective strategies from the literature. There are very few review articles focusing on SD, for instance, Ike et al.[13] emphasized understanding the SD mechanism and its suppression in electrochemical SCs and hybrid SCs. In another perceptive review, Andreas[24] touched upon some important aspects such as the theoretical background, identification of SD mechanism and future directions. Recently, the work of Liu et al.[25] have sufficiently reviewed the SD mechanism and different strategies of suppression, however, recent important developments and comprehensive description of strategies are missing.

Herein, we updated an SD mechanism by referring to recently published important contributions. Furthermore, different strategies have been reviewed and classified based on their employment made not only on materials but also on device level to mitigate the SD. We discussed mitigation strategies, their design, underlying principle, mechanism and corresponding SD performance in detail. Moreover, the summary and prospects in this field have been provided.

Self-Discharge Mechanism

The SD of a conventional capacitor is governed by the equation $V = V_{initial}e^{\frac{-t}{RC}}$ where V, $V_{initial}$, R and C are potential difference, initial voltage, ohmic resistance and capacitance, respectively. In this case, the SD process is completed within microseconds that leads to negligible retention of energy. The RC is the time constant which is the intrinsic property of the capacitor that decides the value of SD.[26] However, in SCs, the SD mechanism involves mainly three processes, (1) ohmic leakage between the electrodes of a full cell, (2) parasitic faradaic reactions on the electrode surface and (3) the charge redistribution.

Self-discharge due to ohmic leakage.—The ohmic leakage between the electrodes is the least discussed mechanism because it is originated due to the faulty construction of the cell (Fig. 1a). This can be avoided by eliminating the resistive pathways which connect the positive and negative electrodes. This can be easily identified by modeling the SD profile using the equation, $\log\left(\frac{V_t}{V_i}\right) = \frac{-t}{RC}$. As shown in Fig. 1d, if the plot of $\log\left(\frac{V_t}{V_i}\right)$ versus the time (t) is a straight line, the main contribution to SD will be due to the ohmic leakage.

Self-discharge due to parasitic faradaic reactions.—In this type, SD takes place due to the oxidation and reduction reactions on the charged electrode surface that lead to the discharge of the electrode and the overall cell (Fig. 1b). This can be easily understood by the following reactions at positive and negative carbon electrode surfaces (C) in sulfuric acid.[24]

[z]E-mail: jagadaleajay99@gmail.com

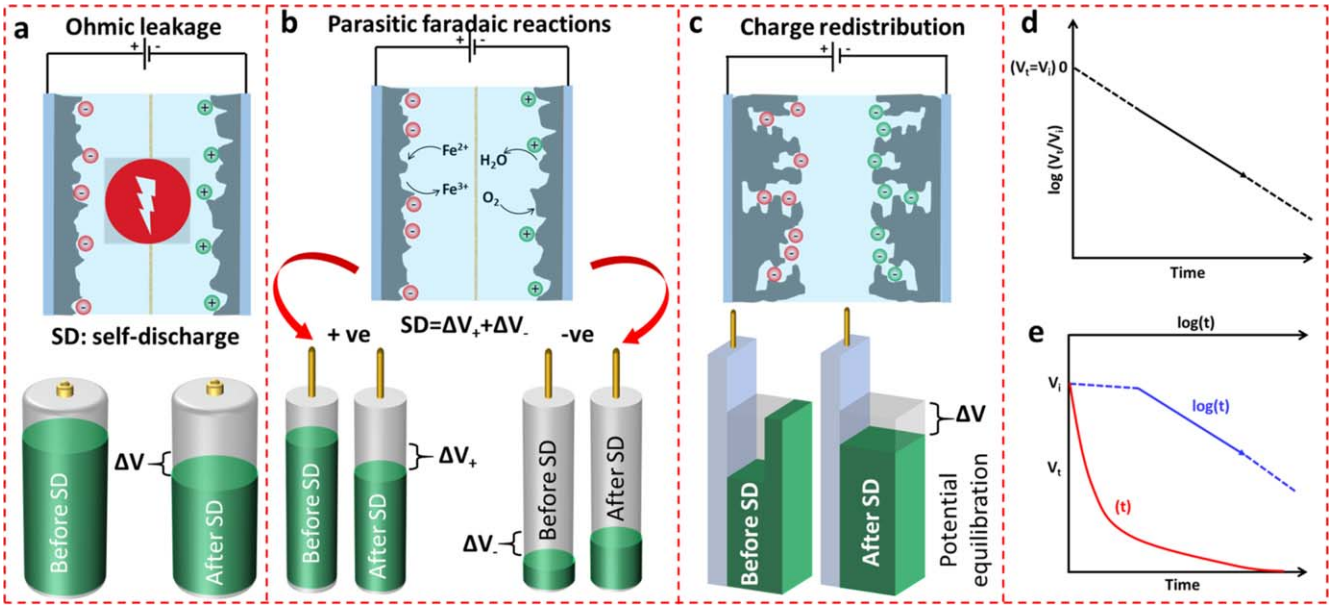

Figure 1. Schematic of different self-discharge mechanisms involved in SCs.

$$\text{Positive electrode: } C^{+}(\text{surf})HSO_4^{-}(\text{ads}) + Fe^{2+}(\text{aq}) \rightarrow Fe^{3+}(\text{aq}) + C(\text{surf}) + HSO_4^{-}(\text{aq}) \quad [1]$$

$$\text{Negative electrode: } 4C^{-}(\text{surf})H^{+}(\text{ads}) + O_2(\text{aq}) \rightarrow 2H_2O(\text{l}) + 4C(\text{surf}) \quad [2]$$

Since the electrons need to be transferred through the double layer or the reacting species need to be diffused toward the electrode surface, this mechanism exhibits a rate-limiting step. The former can be categorized as an activation-controlled mechanism and the latter one is the diffusion-controlled mechanism. These mechanisms can be identified by using the models given by Conway and others.[24,27,28] During an activation-controlled SD, the potential (V_t) is related to the time (t) as shown in Eq. 3,

$$V_t = -\frac{RT}{\alpha F}\ln\frac{\alpha F i_0}{RTC} - \frac{RT}{\alpha F}\ln\left[t + \frac{C\tau}{i_0}\right] (3) \quad [3]$$

where R, T, α, F, i_o, C and τ are gas constant, temperature, transfer coefficient, Faraday's constant, exchange current-density, interfacial capacitance and the integration constant, respectively. As shown in Fig. 1e, the plot of SD potential versus the log(t) depicts a linear drop after a plateau.[24] Besides, during the diffusion-controlled SD, the potential linearly drops with respect to the square root of the SD time as related below,

$$V_t = V_i - \frac{2zFAD^{\frac{1}{2}}\pi^{-\frac{1}{2}}c_0}{C}t^{\frac{1}{2}} (4) \quad [4]$$

where V_i, z, D, c_o and A are initial charging voltage, charge, diffusion coefficient, initial concentration of the reacting species, and the electrode area. It is observed that the presence of redox species or transition metal ion impurities such as Fe, Mn and Ti ions in the electrolyte increases the SD and the leakage current of the SCs. In this case, the SD mechanism involved is mostly shuttle type, in short, impurity species (e.g. Fe^{2+}) are oxidized (Fe^{3+}) on the positive electrode and further diffused toward the negative electrode and are reduced. In this process, the potentials of positive and negative electrodes decrease as shown in the schematic of Fig. 1b. Apart from this, during charging-discharging, the impurity ions slowly penetrate to the positive electrode crystal lattice that deteriorates the cycle life of the positive electrode and thereby the performance of the device.[14,29]

Self-discharge due to charge redistribution.—As a representative example illustrated in Fig. 1c, when porous or pseudocapacitive electrodes are charged, the outer surface of the electrode charges rapidly as compared to the inner surface. The potential of the outer electrode surface reaches quickly to the desired value than the potential of the bulk electrode. When the charging process is stopped, charges start moving to equilibrate the potential through the electrode that leads to an SD. This process is called charge redistribution.[24] The charge redistribution SD profile has different shapes that depend on the size and shape of the pores and the distribution of potential in the electrode. It has been theoretically and experimentally verified that the charge redistribution has two stages, fast diffusion and slow voltage decay. In the fast diffusion stage, SC loses energy rapidly due to the concentration gradient-driven redistribution. This can be avoided by further charging or applying a small current.[30,31]

Since all the mechanisms are simultaneously present, the SD is a complex process. It is important to identify the mechanism involved in the SD and develop different strategies to minimize it. To better understand the type of SD mechanism involved in particular SC, the deconvolution of different mechanisms can be performed using non-linear fitting of experimental data.[16,23,32–35]

Strategies to Mitigate Self-Discharge

Different strategies have been employed on materials and device levels to mitigate the SD of SC via modification of electrode, electrolyte, separator and the device configuration. As shown in Fig. 2, we have classified these strategies and their design, underlying principle, mitigation mechanism and SD performance have been discussed in the subsequent sections.

Electrode modification.—The faradaic reaction of impurities on the electrode surface is one of the major reasons for SD. In a typical example of an EDL capacitor, when the capacitor is charged, impurities cause an SD during which electrons are transferred through the double layer. This electron transfer can be blocked and thereby SD by simply coating an ultra-thin layer of insulating

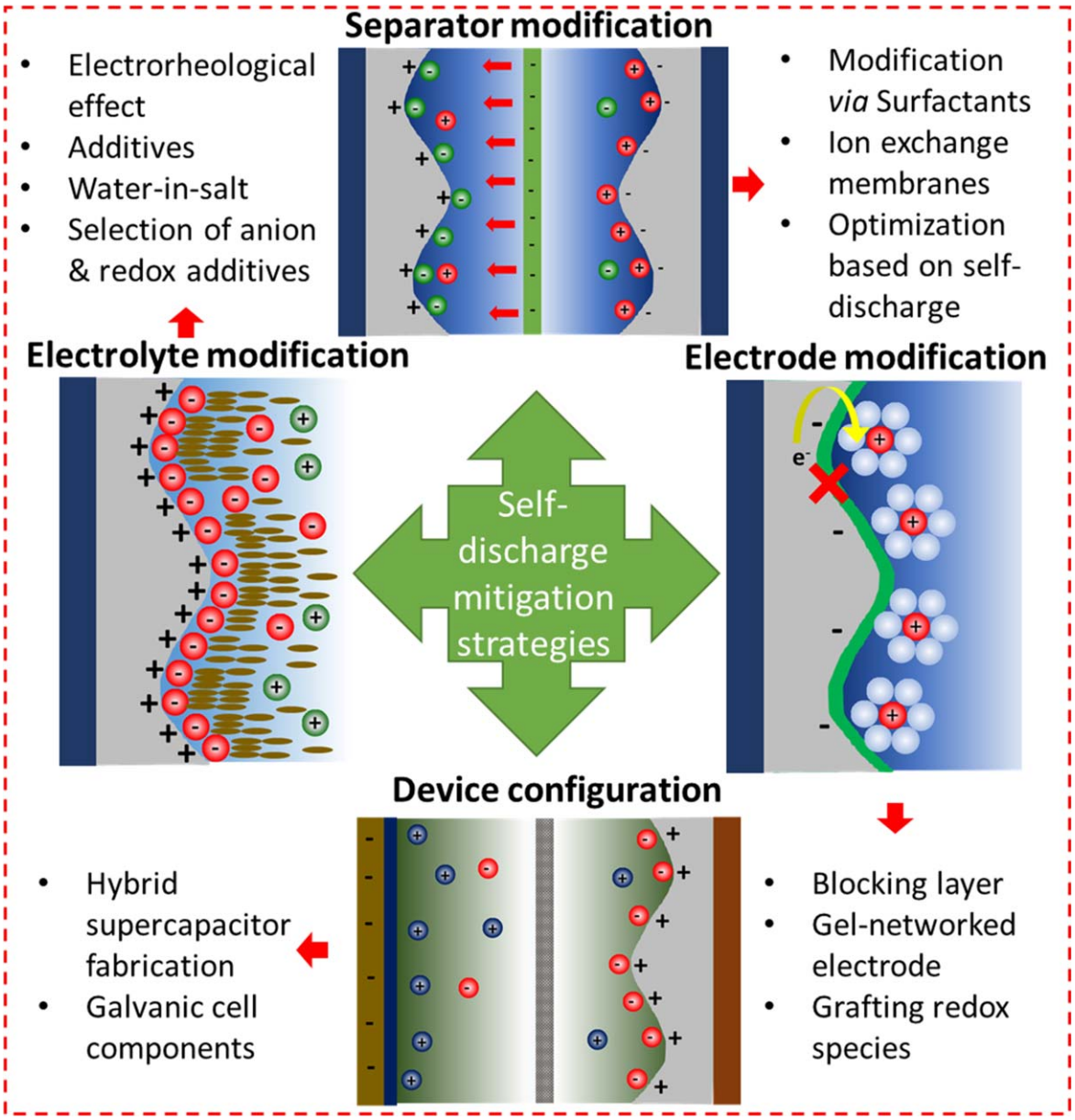

Figure 2. Schematic classification of different strategies to mitigate self-discharge.

material. To avoid SD contribution from the faradaic or the electron transfer reactions at the electrode surface, Tevi et al.[36] coated an ultra-thin layer of poly (p-phenylene oxide) (PPO) on activated carbon as a blocking layer (Fig. 3a). A symmetric SC was fabricated using PPO-coated activated carbon electrodes and (1 M TBAP) propylene carbonate electrolyte. It is found that the blocking layer reduces the SD significantly. The SC with blocking layer demonstrated 17% more voltage retention after 1 h as compared to the SC without coating. This can be an effective strategy to suppress SD, however, the specific capacitance, energy and power densities were compromised after coating. The authors recommended using an ultra-thin coating of PPO to avoid capacitance loss. Moreover, the same group developed an analytical model to explain the SD behavior of the SCs with different thicknesses of the blocking layer by considering the rate constant of the faradaic reactions and the tunneling of electrons through the blocking layer. Based on the particular application, one can predict the optimized thicknesses of the blocking layer. Besides, this model also explicates the effect of thickness of the blocking layers on the capacitive reduction and the energy loss.[37] Another way of reducing SD is to avoid electrolyte decomposition by adjusting the potential of zero charge (PZC) of individual electrodes. The potential window of the SC can be widened by shifting PZC of individual electrodes to a suitable value. Xiong et al.[38] prepared an o-benzenediol functional group grafted carbon electrodes via amido bond to adjust the PZC. The amido bond facilitates efficient charge transfer from the grafted molecule to the carbon electrode and also avoids cross-diffusion of the species. Two SCs were fabricated with and without o-benzenediol functional group grafting on the electrodes. The SC with grafted electrodes demonstrated slower SD (4 h) as compared to the one without grafting (1.9 h).

The introduction of redox additives into the electrolyte is one of the promising strategies to enhance the energy density of the SC. Usually, redox electrolytes in SC weakly interact with electrode surface that leads to poor capacity performance and fast SD. Sun et al.[39] grafted $Fe(CN)_6^{4-}$ groups on the surface of Co_3O_4 to create a synergistic interface between the electrode and the redox electrolyte, suppressing the SD substantially. In their work, Co_3O_4 (CO) nanowires were grown on carbon cloth using the hydrothermal method. The so-called PCO nanowires were prepared by heat-treating

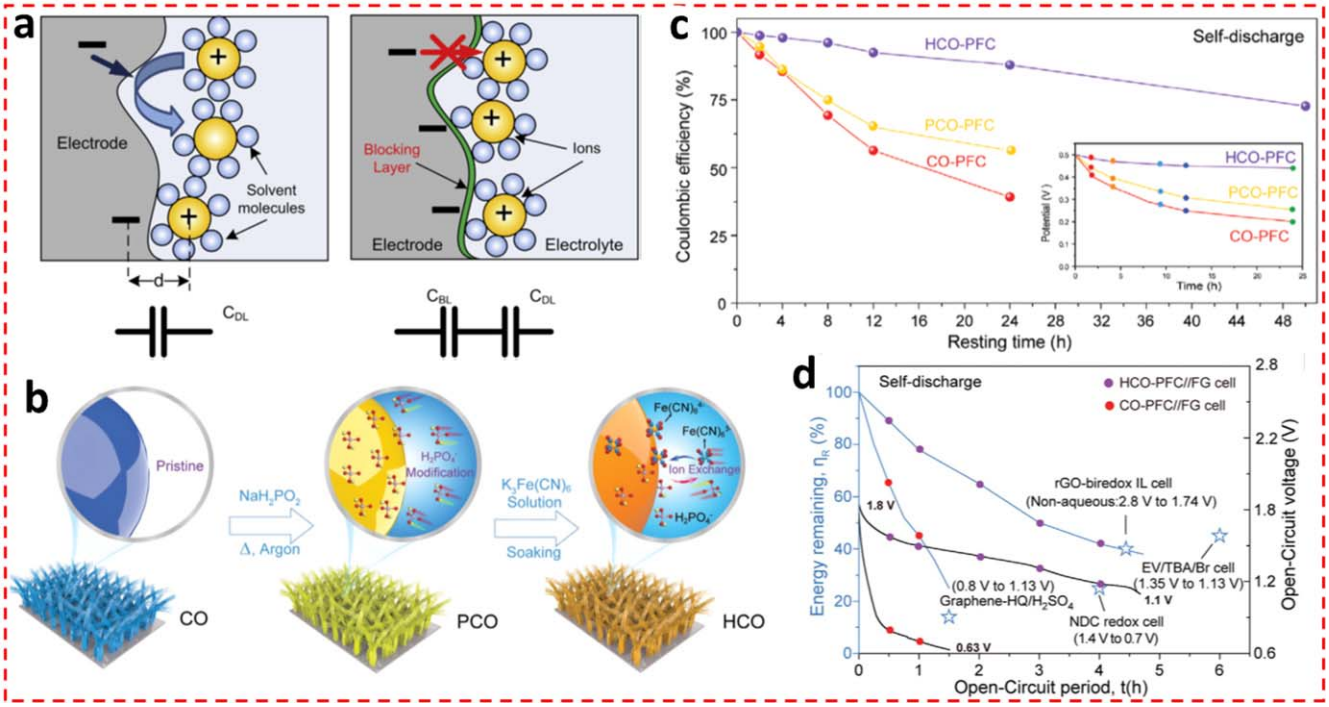

Figure 3. (a) Inhibition of self-discharge through thin insulating blocking layer, reproduced with permission from Ref. 36, (b) illustration of preparation process of PCO and HCO nanowire arrays, (c) self-discharge performances of HCO-PFC, HCO-KOH and CO-PFC in the three-electrode system and (d) variation of energy retention and open-circuit voltage with time of HCO-PFC//FG and CO-PFC//FG SCs, reproduced with permission from Ref. 39.

as grown CO NWs arrays along with NaH_2PO_2 under an inert atmosphere. These phosphate ions-modified Co_3O_4 NWs subjected for ion exchange to get HCO NWs (Fig. 3b). The SD study was performed using the three-electrode system in which CO, PCO and HCO were used as a working electrode, Pt was used as a counter electrode and bare 6 M KOH and 6 M KOH-0.06 M potassium ferricyanide ($K_3Fe(CN)_6$) (PFC) were used as electrolytes (Fig. 3c). In this case, the SD resulted owing to the shuttling of redox couples [$Fe(CN)_6^{3-}/Fe(CN)_6^{4-}$] toward the opposite electrode. As shown in the inset of Fig. 3c, a slower discharge of the HCO electrode was observed. The slow SD is attributed to the fact that the redox-active $Fe(CN)_6^{3-}$ species are well adsorbed and confined on the surface of the HCO electrode. Furthermore, asymmetric devices were fabricated using Fe_2O_3/graphene (FG) as a negative electrode and devices were subjected to an SD test. The HCO-PFC//FG SC retained 38% of full energy after 4.7 h, however, CO-PFC//FG could retain only 24% of full energy after 1.5 h (Fig. 3d). The authors evidenced that layers of PFC are confined around the HCO surface through dipole-dipole interactions, suppressing the cross-diffusion and boosting the SD performance. In another work, Wang et al.[40] fabricated SC based on PANI-gel network electrodes and bi-redox salt-containing (MIm^+-TEMPO-Br^-) electrolyte. The SD issue associated with this redox-active electrolyte is addressed by utilizing PANI-gel network modified carbon paper electrodes. This networked electrode prevented the cross-diffusion of bi-redox electrolyte and thereby the SD. It was claimed that the coupling of bi-redox ions during the doping/de-doping process of PANI mitigates further SD via an additional electrostatic effect. In another work, Zhang et al.[41] prepared hierarchically porous carbon (HPC) electrodes via sol-gel self-assembly method at various concentrations of surfactant, cetyltrimethylammonium bromide (CTAB) (from 0 to 0.55 mol l^{-1}). To investigate the effect of surfactant on the self-discharging characteristics of the SCs, different symmetric SCs were fabricated and subjected to SD tests. The SC fabricated with a CTAB concentration of 0.55 mol l^{-1} showed lower SD. Although the authors identified the self-discharging mechanisms involved, the role of CTAB in preparing HPC electrodes was ambiguous.

Electrolyte modification.—Since the electrolyte is one of the important contributors to SD, much work has been performed on modifying electrolytes for suppressing SD. Recently, the electro-rheological (ER) effect is considered as one of the important approaches to suppress SD in SCs. The ER effect is nothing but the change of the rheological properties of the fluid under the influence of the electric field. The ER fluid contains very small non-conducting but electrically active particles in an electrically insulating fluid. When the electric field is applied, these dispersed particles align themselves in the field direction, leading to a change in the rheological properties of the electrolyte and thereby the charge redistribution and the ionic diffusion processes. Recently, Xia et al.[16] used 4-n-pentyl-4′-cyanobiphenyl (5CB) molecule-based ER electrolyte to suppress the SD. In that work, SC was fabricated using activated carbon electrodes and the triethyl methyl ammonium tetrafluoroborate ($TEMABF_4$) in acetonitrile electrolyte. The 5CB was added to the electrolyte at a volume ratio of 1:49. As shown in Fig. 4a, when the capacitor is charged, the ionic diffusivity is greatly reduced that diminished a charge re-distribution and ionic diffusion away from the electric double layer, leading to a suppressed SD and leakage current. Figs. 4b and 4c demonstrate the SD profiles of SCs fabricated with and without 5CB molecule containing electrolyte, respectively. It is seen that the presence of 5CB enhances the SD performance of the SC by 6-fold. From the simulation results, it is found that the contribution to the SD is mainly from the faradaic and diffusion processes which have been efficiently suppressed by using the 5CB molecule. However, the addition of liquid crystals in the electrolyte compromises the capacitive performance of the SC. To avoid this, it is highly recommended to optimize the content of liquid crystals in the electrolyte. In such work, Haque et al.[42] fabricated symmetric SCs by using activated carbon fabric electrodes and the aqueous solution of 1 M Li_2SO_4 electrolytes. It is seen that the addition of a very small amount of liquid crystal (2 wt%) in the electrolyte suppresses SD significantly without the expense of capacitive and cyclic stability performances.

Recently, all-solid-state SCs attracted great interest because of their exceptional role in wearable electronics.[44,45] However, most of the

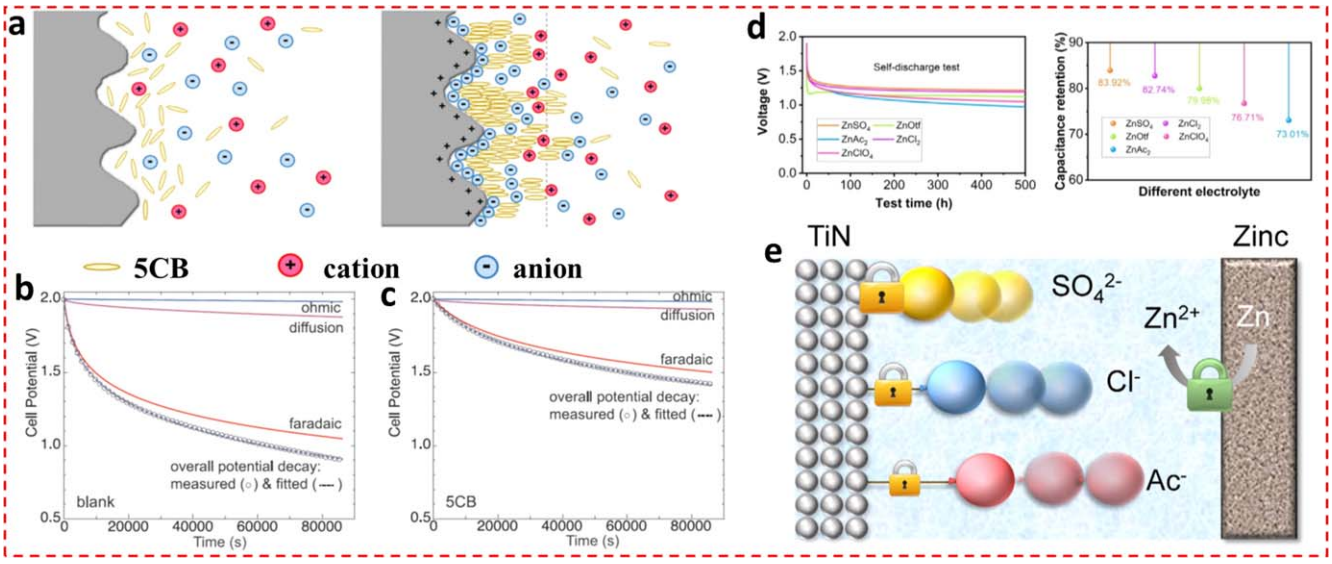

Figure 4. (a) The electrode/electrolyte interface of the electric double layer-type electrode with 5CB added electrolyte at charged and discharged states, (b)–(c) variation of open circuit potential of SCs with and without the 5CB and deconvolution of different contributions, (a)–(c) reproduced with permission from Ref. 16, (d) Self-discharge performance of Zn-TiN capacitors in different electrolytes with their capacitance retentions after test, (e) schematic of different self-discharge behaviors of zinc ion capacitors, (d), (e) reproduced with permission from Ref. 43.

solid-state SCs self discharge rapidly within a few minutes.[46,47] The SD of all-solid-state SC can be suppressed by using the polymer gel electrolyte to retard the ionic transport.[48] For instance, Li et al.[49] prepared polyacrylamide hydrogel electrolyte-based SCs and compared their SD and leakage current characteristics with other polyelectrolytes (e.g., PVA/LiCl and PVA/H_3PO_4). The SC based on polyacrylamide hydrogel electrolyte demonstrated slow SD as compared to other polyelectrolytes. The authors claimed that the improved SD performance was attributed to the slow charge redistribution taking place in the 3D porous polyacrylamide hydrogel electrolyte. The mechanism behind the SD was not properly identified by using different models discussed earlier. In another work, Gong et al.[50] found that the use of ionogel electrolyte improves the SD performance of the (FeOOH/PPy@CF//MnO_2@CF) asymmetric SC. The ionogel electrolyte ([EMIM][TFSI]/FS) was synthesized by adding fumed silica into ionic liquid [EMIM][TFSI] followed by stirring. The authors claimed that the SD is originated due to the ion migration resulted from the combination of potential field and the concentration gradient. However, in that work, the role of ionogel and the SD mechanism was not elucidated. In similar work, Fan et al.[51] prepared a redox-active ionic liquid (IL)-based ionogel electrolyte (IGE) for all-solid-state SC (ASSC). The IGE was comprised of 1-butyl-3-methylimidazolium iodide (BMIMI) IL, poly(vinylidene fluoride-co-hexafluoropropylene) (PVDF-HFP) and carbon nanotubes (CNTs). Two all-solid-state SCs were fabricated with and without CNTs and their SD profiles were studied. It is found that the SC with CNTs-based IGE showed slower SD with voltage retention of 0.79 V after 5 h. Authors claimed that the slower SD is attributed to the presence of CNTs that adsorb I^{3-} ions on their surface and prevent their self-diffusion towards the negative electrode. Moreover, the same group[52] fabricated quasi-solid-state SC by incorporating carbon nanotubes into redox-active ionic liquid-based gel polymer electrolyte. A redox-active gel polymer electrolyte (GPE) was prepared by adding 1-butyl-3-methylimidazolium bromide (BMIMBr) ionic liquid (IL) and CNTs into poly(vinyl alcohol) (PVA) solution followed by the addition of Li_2SO_4. In their research, three activated carbon-based SCs were fabricated by using three different electrolytes such as PVA-Li_2SO_4, PVA-Li_2SO_4-BMIMBr and PVA-Li_2SO_4-BMIMBr-CNTs and their SD performance was investigated. From the SD profile, it is seen that, after 5 h, the voltages of SCs were 1.18, 0.62 and 0.70 V, respectively. The enhanced performance is attributed to the addition of CNTs into GPE which adsorbs Br^{3-} species and avoids their diffusion towards the negative electrode, further preventing SD.

Employing water-in-salt electrolytes is also an effective strategy to mitigate the SD of SCs. The water-in-salt electrolyte is nothing but preparing a super-concentrated solution with a salt-to-water ratio larger than unity.[53] Previously, Avireddy et al.[54] prepared potassium acetate-based water-in-salt electrolyte to suppress the SD. The asymmetric SC was fabricated using 2D MXene (Ti_3C_2) as a negative electrode, α-MnO_2 as a positive electrode and 21 m potassium acetate as a water-in-salt electrolyte. Initially, within 30,000 s, the cell voltage dropped from 2.2 to 1.5 V, demonstrating 68% voltage retention. The authors claimed that the improved SD is attributed to the diffusion limitation of charges at the electrolyte-electrode interface in the water-in-salt electrolyte.

The type of anions of the electrolyte has a substantial effect on the SD ability of the SCs. Utilizing a suitable electrolyte is a rational strategy for suppressing SD. Huang et al.[43] recently fabricated hybrid Zn ion capacitors with different types of anions containing electrolytes including $ZnSO_4$, $ZnCl_2$, ZnOtf, $ZnClO_4$, and $ZnAc_2$. The Zn ion capacitor was fabricated using Zn as anode and TiN as the cathode. Figure 4d shows SD profiles of all hybrid SCs fabricated with different electrolytes, indicating voltage retention up to 0.97 −1.22 V after 500 h. The capacitance retentions were 83.92, 82.74, 79.98, 76.71, and 73.01%, respectively after the resting time of 500 h (Fig. 4d). It is observed that the SD performance of the $ZnSO_4$-based Zn ion capacitor was superior. Authors attributed this to the more negative adsorption energy of the SO_4^{2-} anion on the surface of TiN cathode. As illustrated in the Fig. 4e, the $ZnSO_4$ based zinc ion capacitor mitigate the SD process for two reasons; 1) the sluggish kinetics of Zn conversion into Zn^{2+} ions and 2) the more negative adsorption energy of SO_4^{2-} anion on the surface of TiN. Earlier, similar work was performed on activated carbon-based symmetric SCs by Zhang et al.[55] They fabricated hierarchically porous carbon-based symmetric SC by using different electrolytes including $(NH_4)_2SO_4$, Na_2SO_4, H_2SO_4 and KOH, and the effect on SD was investigated. The SD performance of neutral 2 M Na_2SO_4-based SC was found superior as compared to other SCs.

The selection of appropriate redox-active electrolytes is also an efficient way to suppress SD without the expense of capacitive performance. For instance, Luo et al.[56] used Cu^{2+} active electrolyte to enhance the capacitive performance of the PANI/rGO based SC without sacrificing the SD performance. The notion behind choosing the Cu^{2+}/Cu couple was its relatively lower potential (0.1 V vs SCE) on the rGO electrode. Different devices were fabricated with and

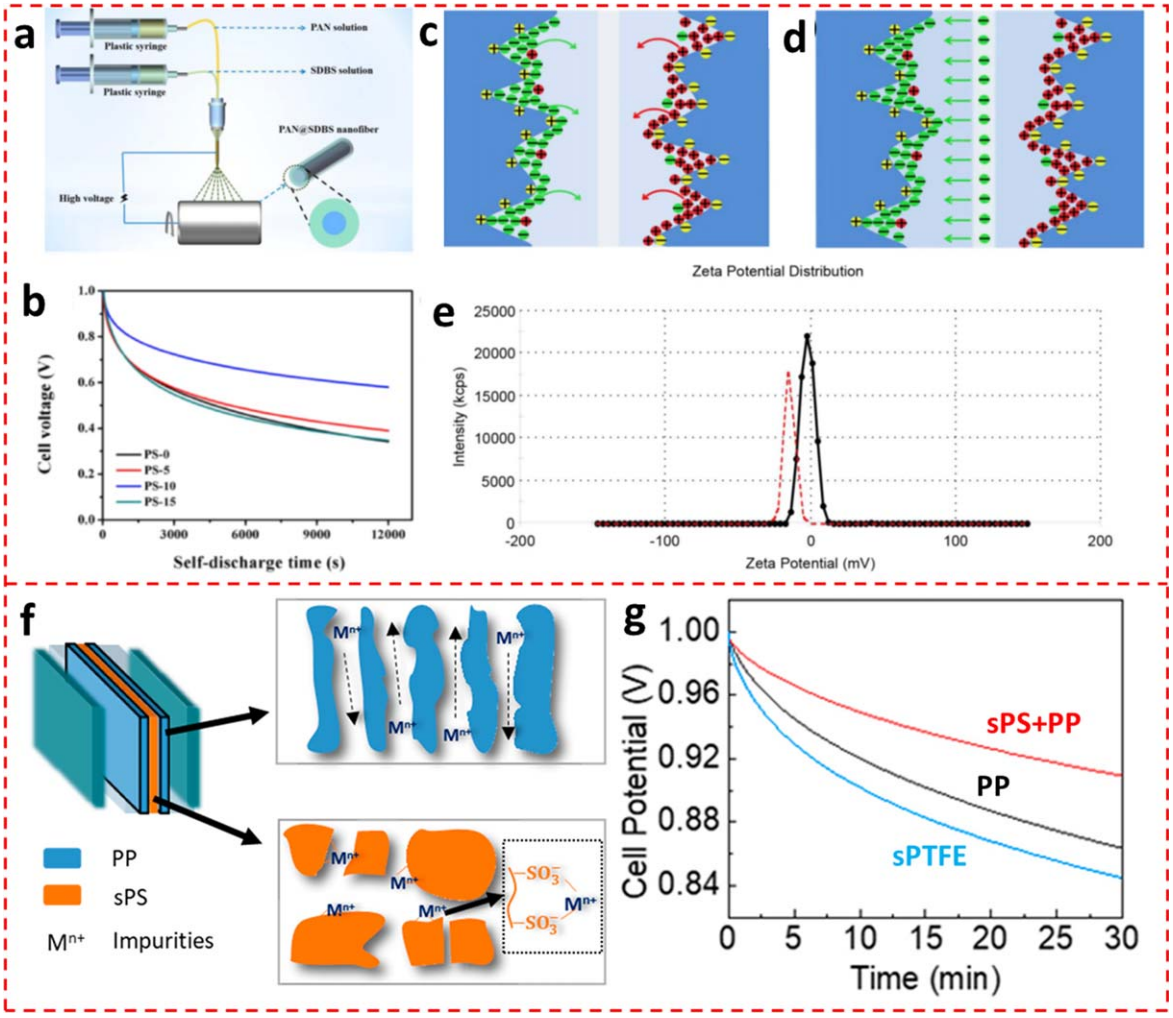

Figure 5. (a) Schematic of co-axial electrospinning process, (b) self-discharge profiles of SCs based on different PAN@SDBS membranes (c)–(d) schematic of SC with bare nanofiber membrane and PAN@SDBS membrane separators, (e) zeta potential distribution of bare nanofiber membrane and PAN@SDBS (10%) membrane separators, (a)–(d) reproduced with permission from Ref. 61 (f) schematic of the capture of cationic impurities, (g) self-discharge profiles of SCs with different separators, (f), (g) reproduced with permission from Ref. 62.

without the addition of the $CuSO_4$ additive. In terms of SD, an SC with Cu^{2+} active electrolyte and the PANI/rGO anode outperformed the other devices. It is seen from the study that the incorporation of Cu^{2+} doses did not accelerate the SD process, instead, during the charging process, Cu^{2+} species reduce to form insoluble Cu metal and get immobilized, thereby mitigating the shuttle effect. In similar work, Wang et al.[57] introduced PVA in the Cu^{2+} containing redox-active electrolyte to suppress the SD. They fabricated SC with $CuCl_2$/PVA/H_2SO_4 and PVA/H_2SO_4 as the electrolytes for positive and negative electrodes, respectively. It is seen that the PVA containing SC demonstrates excellent SD performance by declining to half of its initial potential after a relatively long time (18465 s) as compared to SC without PVA. Authors claimed that the suppressed SD attributes to the moderate kinetics and ion crossover rate of PVA-based electrolyte. In another interesting work, Wang et al.[15] used the so-called "playing mud pies" strategy to mitigate SD via the preparation of bentonite clay@ionic liquid-based solid-state electrolyte (BISE). A blend was prepared by simply mixing bentonite clay and thermoplastic polyurethane in N, N-dimethylformamide solvent. Furthermore, SCs were fabricated using activated carbon electrodes and solid-state electrolyte prepared via soaking self-standing films of the blend into ionic liquid ($EMIMBF_4$). Interestingly, this SC showed a very low SD with voltage decay of only 28.9% after 60 h. This solid-state electrolyte is found beneficial in three ways; (1) its excellent mechanical strength avoids internal short circuit, (2) small cations between bentonite clay are replaced by impurity ions, thereby diffusion of impurities is inhibited via confinement effect and (3) electrolytic anions selectively penetrate through the silicon-oxygen bonds.

The addition of surfactants in the electrolyte is also an effective strategy to reduce SD in SCs. Recently, in SCs based on $MnFe_2O_4$ colloidal nanocrystal cluster, the effect of surfactants added in the electrolyte solution of $LiNO_3$ on SD characteristics was examined. Different surfactants were chosen such as sodium dodecyl sulphate (SDS), Triton-X-100 and poly(ethylene glycol)-block-poly(propylene glycol)-block-Poly(ethylene glycol) (P123). The SD of SDS-based SC was found slower.[58] However, the mechanism behind the mitigation was not clearly explained. In another study, it has been observed that if the electrolyte is modified with a non-ionic surfactant, for instance, Triton X-100, the SD of the SC can be suppressed. This is attributed to the orientation of the Triton X-100. It is oriented in such a way that the benzene ring faces the electrode (carbon) surface and the alkyl chain is left into the electrolyte. This chain acts as a micro-insulator and further hinders the leakage current and thereby the SD.[59]

Separator modification.—One of the major contributions to SD is the shuttle effect, normally observing in redox-active electrolyte-based SCs. The shuttle effect can be suppressed using an ion-exchange membrane or via separator modification.[60] For instance,

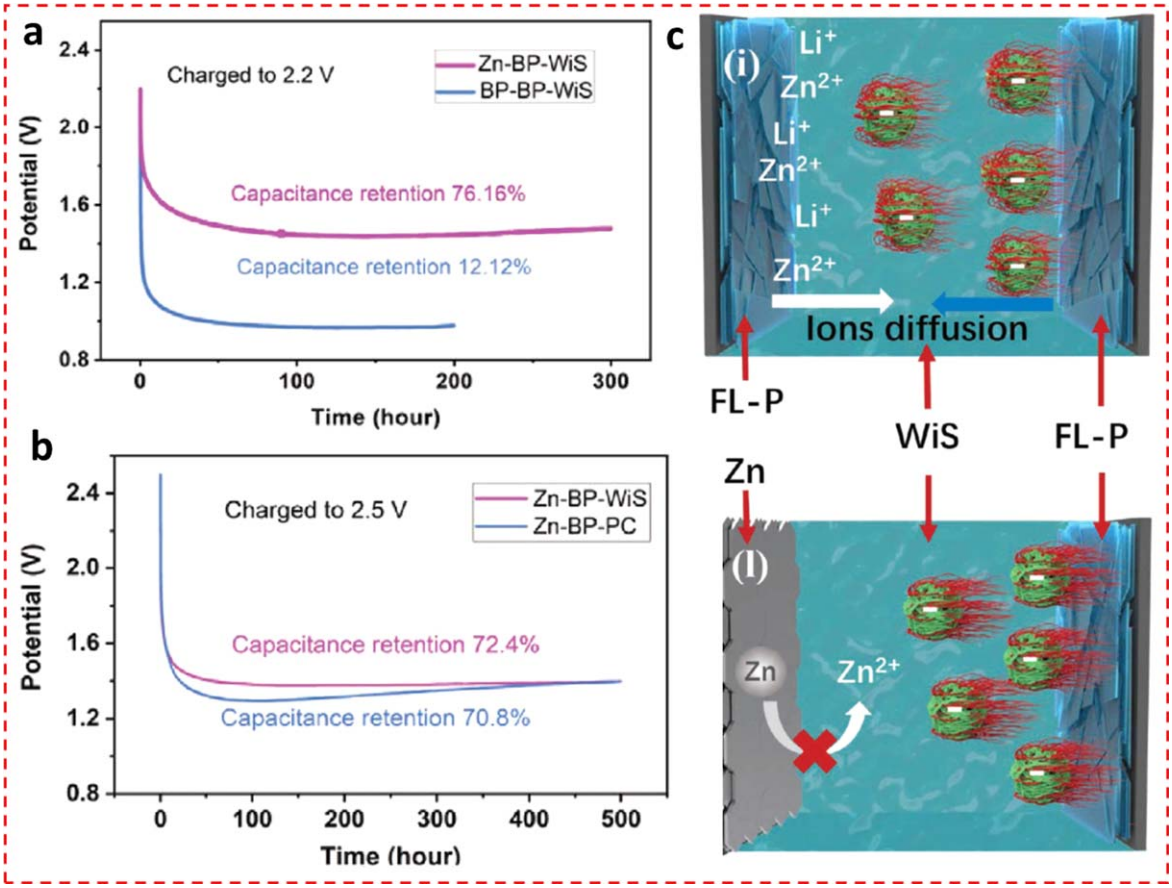

Figure 6. Self-discharge curves of (a) Zn-BP-WiS and BP-BP-WiS, (b) Zn-BP-PC and Zn-BP-WiS SCs, (c) illustration of FL-P-based symmetric SC and zinc-ion hybrid SC in the charged state, (a)–(c) reproduced with permission from Ref. 65.

Peng et al.[61] recently prepared polyacrylonitrile (PAN)@sodium dodecylbenzene sulfonate (SDBS) nanofibers membrane using electrospinning method and used as a separator in the activated carbon-based SC (Fig. 5a). The effect of concentration of SDBS solution and thereby the microstructure of the membrane on SD was investigated. The PAN@SDBS membrane prepared at 10% SDBS was found suitable to suppress the SD (Fig. 5b). Figures 5c and 5d show an SC with and without PAN@SDBS core@sheath nanofibers membrane. When SC was charged, anions and cations from the electrolyte were adsorbed on the negative and positive electrodes, respectively. Since this is a thermodynamically higher energy state, the system will find some means to come to the lower energy state. Therefore, due to the concentration gradient, adsorbed ions from the electrode tend to move toward the bulk electrolyte solution and SD takes place. The sheath material was made of SDBS, exhibiting Na^+ ions those release in the electrolyte, leaving a negative charge on the separator. While diffusing, anions experience a repulsive force of the separator, leading to a suppressed migration. On the other side, the diffusion of cations is also suppressed because of the lack of compensation of anions. Figure 5c shows the zeta potential measurement of membranes with 0 and 10% SDBS, indicating the negative charge of the separator. In another study, Wang et al.[62] modified a polypropylene separator by incorporating a cation-exchange resin (purolite). They fabricated SCs with redox-active PEDOT (poly(3, 4-ethylenedioxy-thiophene) electrodes and three different separators such as polypropylene (PP), sulfonated-fluoropolymer (sPTFE) and polypropylene-sulfonate polystyrene resin (sPS + PP). As shown in Fig. 5f, the sPS+PP separator inhibits the movement of impurity ions by binding them to the polymer matrix and an equivalent number of resin cations are released as an exchange reaction. It is observed that the sulfonate groups in polystyrene resin can mitigate SD via two processes, (1) by reducing a concentration of redox impurities via ion exchange adsorption and 2) decelerating the diffusion of impurities. Thus, the purolite with sulfonated end groups was found to be an exceptional cation adsorbent, suppressing the SD phenomenally (Fig. 5g).

Lee et al.[63] used cation exchange membrane (FKS20) to mitigate the shuttle effect of ferricyanide/ferrocyanide ions in the activated carbon-based SCs. The SD characteristics of SCs based on Na_2SO_4 and potassium ferricyanide electrolytes with and without cation exchange membrane have been studied. It is seen that the SD of SCs based on redox-active electrolytes can be effectively suppressed by simply replacing the porous separator with an ion-exchange membrane. Besides, the effect of different types of separators such as nonwoven polypropylene mat, porous polypropylene membrane, Al_2O_3-coated polypropylene membrane, and nonwoven cellulose paper on the SD characteristics of SCs and hybrid SCs have been studied. The hybrid SC with a nonwoven polypropylene separator showed superior SD performance.[64]

Modification of device configuration.—The fabrication of a hybrid SC is also an effective way of mitigating the SD behavior of the SC. Hybrid SC is nothing but a combination of battery and capacitive electrodes in a single device. Unlike the adsorption type electrode (capacitive), the battery-type electrode such as insertion or conversion type has a strong tendency to limit ionic diffusion from the charged electrode to the bulk electrolyte, substantially suppressing the SD. Huang et al.[65] fabricated a hybrid Zn-ion capacitor by using a few-layered phosphorene (FL-P) as cathode and Zn metal foil as the anode. The FL-P was prepared via electrochemical exfoliation of black phosphorus (BP). Two different hybrid SCs were fabricated by utilizing WIS (water in salt) (Zn-BP-WiS) and propylene carbonate (Zn-BP-PC) electrolytes. These devices were kept for SD tests and their performances were compared with

Table I. Capacitive performance along with self-discharge of few individual electrodes and full cell SCs reported so far.

Device configuration Anode/cathode	Electrolyte	Cell voltage (V)	Energy density (Wh kg^{-1})	Power density (W kg^{-1})	Self-discharge (voltage retention (%), time (h))	References
Carbon//carbon	2 M $LiBF_4$: acetonitrile	1–3	5.6	900	26.3, 200	67
$Li_4Ti_5O_{12}$//carbon		2.8–4.2	11	1000	21.4, 200	
PANCF-PANI//PANCF-PANI	1 M H_2SO_4	0–0.6	4.25	1200	20, 10	68
$MnFe_2O_4$–carbon black// $MnFe_2O_4$–carbon black	1 M NaCl	0–1	7.6	11000	—	69
AC//AC	Acrylamide-based polymer gel electrolyte	0–1	3.24	500	—	
$MnFe_2O_4$@C//$LiMn_2O_4$	Aqueous $LiNO_3$	0–1	10	—	15, 1.7	70
HPC//HPC	6 M KOH	0–1.2	11.54	10580	—	55
AC//AC	PVA-PVP-H_2SO_4- Methylene blue GPE	0–1	10.3	246	31, 24	71
CSC//CSC	6 M KOH	0–1	—	—	7.5, 11	72
NENCs-600// NENCs-600	6 M KOH	0–1	—	—	70, 11.6	73
B-Si/SiO_2/C//PSC LIC	$LiPF_6$ in EC: DEC: DMC	2–4	128	1229	82, 50	74
GHG//GHG	0.1 M sulfonated polyaniline + 4 M H_2SO_4	0–0.8	—	—	~22, 14	75
OMC-600//OMC-600	6 M KOH	0–1.1	—	—	69, 12	76
$Co(OH)_2$	1 M LiOH	0–0.8 vs Ag/AgCl	—	—	50, 30	77
MNG//MNG	$EMIMBF_4$	0–3	41	100	50, 3.4	78
rGO/PANI-PSS// rGO/PANI-PSS	PVA-H_2SO_4gel	0–1	30.1 mWh/cm^3	0.37 W cm^{-3}	~21, 24	79
rGO/PPy NP//rGO/PPy NP	PVA-H_2SO_4gel	0–1	26.4 mWh/cm^3	99.4 mW cm^{-3}	~21, 24	80
rGO/PPy NT//rGO/PPy NT	PVA-H_2SO_4gel	0–1	8.32 mWh/cm^3	0.12 W cm^{-3}	~22, 24	81
Glu-Zn-2//Glu-Zn-2	6 M KOH	0–1	—	—	63, 24	82
CNFs/PANI//CNFs/PANI	PVA-H_2SO_4gel	0–0.8	4.4	103	22, 24	83
Si-VACNFs//TiO_2-VACNFs	LiTFSI + EC: DMC PVdF-HFP gel	0–2.2	127	83	79.5, 200	84
BDA/rGO//BDA/rGO	$BMIMBF_4$	0–3.5	34	425	57, 24	85
PEDOT + Lignin/PAAQ	0.1 m $HCLO_4$	0–0.7 vs Ag/AgCl	—	—	~68, 24	86
3D Ni-$NiCo_2S_4$//N-doped rGO	PVA-KOH gel	0–1.4	5.33 mW h cm^{-3}	855.69 mW cm^{-3}	50, 5.5	87
AC//AC	PVA/KOH/carbon black	0–1.4	15.5	700	50, 15	88
NZSC-4//AC	PVA-KOH gel	0–1.7	36.17	850	60, 24	89
FeOOH-CNFP//Ni–Mn hydroxide-carbon	1 M KOH	0–1.8	1515mWh cm^{-2}	9 mW cm^{-2}	55.5, 10	23
PNG//PNG	$[BMIM]PF_6$	0–3	163.8	600	73.2, 10	90
Ni-Mn LDH-MnO_2//AC	1 M KOH	0–1.5	16	15000	66.6, 40	91
3D-G/PANI//3D-G/PANI	PVA-H_2SO_4 gel	0–0.8	14.2 mW h cm^{-3},	3.4 W cm^{-3}	66.25, 4	92
Cotton-CNF + AC//Cotton-CNF + MnO_2	1 M Na_2SO_4	0–1.6	12	—	~75, 8	93
CO_2@C//CO_2@C	$LiCF_3SO_3$-PMMA g	0–1	99	1000	0, 1.66	94
PEDOT//PEDOT			122	1000	13, 1.66	
PEDOT-CO_2@C//PEDOT-CO_2@C			281	1000	18, 1.66	
PEDOP@ MnO_2 based photo-SC	PMMA + ([BuMeIm+] [$CF_3SO_3^-$])/PC	0–0.72	13.2	360	71.4, 0.14	95
$MgCo_2O_4$@PPy/NF//AC	PVA-KOH gel	0–1.6	33.4	320	37.5, 25	96
CO_2 activated AC//CO_2 activated AC	0.75 M NaI and 0.5 M $VOSO_4$ 1 M H2SO_4	0–0.8	3.81	—	8.5, 0.83	97
		0–0.8	2.85	—	41, 0.83	
Co_3S_4@Ni_3S_4//PC HSC	2 M KOH	0–1.6	0.19 mWh cm^{-2}	1.72 mW cm^{-2}	53.12, 12	98
AC-PPY-6// AC-PPY-6	2.5 M KNO_3	0–1.5	12.4	415	69.33, 80	99

Table I. (Continued).

Device configuration Anode/cathode	Electrolyte	Cell voltage (V)	Energy density (Wh kg^{-1})	Power density (W kg^{-1})	Self-discharge (voltage retention (%), time (h))	References
MoS_2@3D-Ni//MoS_2@3D-Ni	PVA/Na_2SO_4 gel	0–1	5.4	—	30, 2	100
N-doped RGO//N-doped RGO	PVA/Na_2SO_4 gel	0–1.2	28.2	—	58.33, 16	101
MnOx/Ni//carbon cloth	1 M KOH	0–1.2	10	1–3	0, 9.7	102
	1 M Na_2SO_4	0–1.6	10		0, 7.3	
CP/PANI//CP/PANI	PVA-H_2SO_4 gel	0–0.8	13.3	80	47.8, 24	103
SiOx@FC//N-doped carbon LIC	1 M $LiPF_6$ in EC: DMC	0–3.7	220	370	82.1, 48	104
Ni-foam	0.5 mmol $K_3Fe(CN)_6$ + 0.5 mmol $K_4Fe(CN)_6$ in 30 mL 2 M KOH	0–0.55 vs Hg/HgO	—	—	80, 12	105
$LiMn_2O_4$	2 M Li_2SO_4	0–1.2	—	—	66.6, 22	106
AC//$NiCo_2O_4$@$Ni_{4.5}Co_{4.5}S_8$	3 M KOH	0–1.5	124.77	1080	50, 26.62	107
RHAC-T//RHAC-T	1 M $Et_4NBFNBF_4$/PC	0–2.5	29.99	25.57	84.4, 24	108
Zn//LDC	Gelatin/$ZnSO_4$ gel	0–1.8	86.8	429.6	77.7, 24	109
YP-80F//Ni_1Co_1-OH	PVA-KOH gel	0–1.6	27.9	13812.9	75, 24	110
AC/Ni-foam//CP/Ni-foam	3 M KOH	0–1.7	43.2	293.1	79, 0.066	111
P-BDD	0.1 M H2SO4	0–1 vs Ag/AgCl	—	—	25.4, 12	112
AC//AC	PVA–Na_2SO_4–$Pyr_{14}Br$ (IL) gel	0–2	33	459.2	46, 4	113
HNCNB//PHNCNB LIC	1 M $LiPF_6$ in EC: DMC	1–4	148.5	250	79.5, 18	114
CSAC//CSAC	PVA-KOH-HQ	−1–1	33.15	689.58	~48, 10	115
V-GHG//V-GHG	2 M $VOSO_4.xH_2O$ + 2 M H_2SO_4	0–1.2	75.7	167.5	47.5, 14	116
PPyCNT5.5// PPyCNT5.5	1 M H_2SO_4	0–0.8	—	—	43.75, 20	117
AC//$NiCo_2O_4$	3 M KOH	0–1.6	16.6	291	99.62, 24	118
CC/$Ni(OH)_2$// CC/CNTs	PVA/H_2SO_4 gel	0–1.8	132.7	27700	17.7, 0.5	119
AC//AC	$LiNO_3$/H_2O-DMSO + HPOM ($H_3PW_{12}O_{40}$)	0–1.8	—	—	38.8, 30	120
PC//PC	1 M $TEABF_4$/AN	0–2.7	0.15 mW h cm^{-2}	5.40 mW cm^{-2}	59.25, 30	121
2D Polymer, P1	H_2SO_4	0–1	112	250	38, 12	122
p(EDOTOH)// p(EDOTOH)	0.1 M NaCl	0–1.75	—	—	38.28, 25	123
CMK-3//PProDOT	(EMIm+$N(CF_3SO_2)_2^-$)+PC + PMMA gel	0–1.5	0.16 mW h cm^{-2}	0.86 mW cm^{-2}	3.33, 0.125	124
MWCNT//MWCNT	PVA + 0.75 KCl+0.3CB gel	0–1	14.16	1.38	60.63, 16.6	125
PC//Co_3O_4@Ni_3S_4	2 M KOH	0–1.6	0.13 mW h cm^{-2}	1.6 mW cm^{-2}	—	126
RGO/N-RGO//RGO/N-RGO	PVA/Na_2SO_4	0–2.2	106.3	5981	22.72, 2	127
AC//AC	PVA–LiTFSI–KBr hydrogel polymer	0–2	34.5	533.7	49.5, 5	128
AC-PS//RGO-S/MnO_2	2.5 M KNO_3	0–1.7	71.74	850	58.8, 72	129
HAC700//HAC700	1 M SBP-BF_4/PC	0–2.7	—	—	84.8, 10	130
α-MnO_2/N&S-rGO//α-MnO_2/N&S-rGO	[DEME][TFSA]/ PVDF-co-HFP	0–4.5	110	550	~28.8, 72	131
NF/CNTs//NF/$CoFe_2O_4$ sphere/PEDOT	3 M KOH	0–1.6	230.4	616	~33.1, 2.7	132
BL-MS//BLMS	PVA/Na_2SO_4	0–1.5	38.79	—	41.3, 2	133
AC//HPCF	2 M $ZnSO_4$	0–1.8	127	—	78.8, 24	134

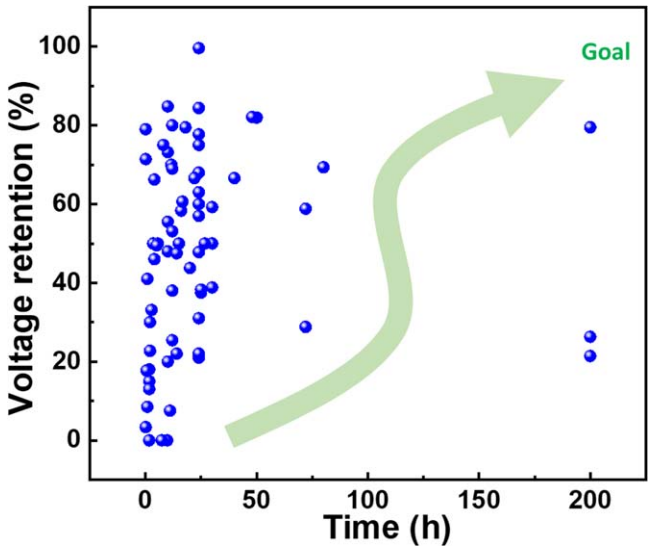

Figure 7. Plot of voltage retentions against a time of SCs reported so far (data extracted from Table I).

symmetric SCs. As shown in Fig. 6a, the Zn-BP-WiS capacitor demonstrated excellent capacitance retention of 76.16% after 300 h of resting. The symmetric BP-BP-WIS showed only 12.12% potential retention after 200 h of resting. As shown in Fig. 6b, the SD performance of the Zn-BP-WiS capacitor was found to be excellent as compared to the Zn-BP-PC capacitor. Authors claimed that the improved performance is attributed to the introduction of the conversion-type zinc anode in the hybrid SC, making a hurdle for adsorbed ions to self-diffuse (Fig. 6c). Also, in symmetric SC, the main driving force for SD is the concentration gradient and the voltage difference. However, in the Zn ion capacitor, there is no cation concentration gradient on the Zn electrode and also the kinetics of adsorbed Zn ion is sluggish for self-diffusion. In another study, Wang et al.[66] assembled SC with galvanic cell components which are expected to generate a micro-current to compensate the SD current. The carbon-based SC fabrication was slightly modified by utilizing copper and zinc current collectors for positive and negative electrodes, respectively. The electrolyte was formed of 1.5 M zinc sulfate soaked in the polyvinylidene fluoride (PVDF)/ lithium trifluoromethanesulfonate (LiTFS) membrane. To compare SD behavior, another SC was prepared with Au as current collectors. The OCV of Au-based SC was retained 55.6% after 810 h. On the other hand, the Cu and Zn-based SC demonstrated huge OCV retention with slight decay after 810 h. Also, it is observed that the OCV was stabilized at 0.85 V and retained 94.4% after one month. Authors claimed that the suppressed SD is attributed to the compensation of current provided by the Cu and Zn galvanic components.

Recently, much work has been performed on testing SD characteristics of individual electrodes or devices. However, these research articles do not focus on the strategic suppression of SD. Table I presents the SD performance of different SCs reported so far along with their energy and power densities. Additionally, Fig. 7 shows voltage retentions of various SC systems after SD. It is seen that the SD of most of the SCs has been tested for 24 h of duration and below. The ultimate goal of this field is to develop SCs with low SD without sacrificing energy, power, and stability performances.

Summary and Outlook

In this review, we explained an SD mechanism in a simplistic way along with the discussion of its identification through mathematical expressions and curve fitting. Different strategies such as modification of electrode, electrolyte, separator and device configuration for mitigating SD have been discussed based on the design, underlying principle, mitigation mechanism and SD performance. Some of the major developments have been pointed out below,

1. The SD has been effectively suppressed by coating an ultra-thin insulating layer, utilizing gel-networked electrodes and grafting redox species on the electrode surface.
2. Utilization of electrorheological fluid additive and water-in-salt electrolyte, as well as a selection of appropriate anions and redox additive containing electrolytes, can be effective ways to suppress SD.
3. To mitigate SD, the separator modification was made via surfactants and ion exchange membranes.
4. Fabrication of hybrid devices by combining merits of battery and SC, and utilizing galvanic cell components have been performed to reduce the SD.

Apart from these achievements, there is much scope in developing SCs with high SD performance. Some of the major issues in the SD characterization and future possible developments of this ignored field have been discussed below,

1. Most of the SD performance data is available for full cells and very few research articles present data of individual electrodes. It is recommended to use a three-electrode system to figure out the SD performance of individual electrodes.
2. It is imperative to first identify the SD mechanism involved in the individual electrodes and develop strategies to mitigate it. The deconvolution of different mechanisms is recommended through which one can understand the contribution of different processes to the SD and strategies can be made accordingly.
3. Applying an ultrathin layer of insulating material on the electrode surface can be an effective strategy, however, it will not be useful for SCs based on redox-active electrolytes, since electron transfer is one of the dominant reactions. Instead, utilizing gel networked electrodes or grafting redox species can be effective.
4. Although the employment of electrorheological fluid suppresses SD substantially, they are adversely affecting the other important SC parameters such as capacitance, cycle life, etc. It is highly recommended to search for novel electrorheological materials and optimize their concentration in the electrolyte to reduce SD without the expense of other useful properties. Using water-in-salt electrolytes can be effective, however, since these are highly concentrated liquids, the cost of the final device may go up. The selection of proper anion-containing electrolytes or redox species can be an effective solution.
5. Using an ion exchange membrane can be effective, however, their high cost will render practicability. Novel and cost-effective ion exchange membranes must be developed and employed as an anti-SD entity in SCs.
6. Fabrication of hybrid SC has great capability of combining anti-self-discharging ability of battery with SCs. Since the selection of anions is imperative, it is recommended to fabricate hybrid SCs with an appropriate electrolyte solution.
7. Additionally, much computational work is anticipated on estimating the adsorption energies of different anions and cations on surfaces of capacitive electrodes at different sites for strategic suppression of SD.

Acknowledgments

ADJ is thankful to the Department of Science and Technology (DST), Govt. of India for financial assistance under the DST INSPIRE Faculty Scheme [DST/INSPIRE/04/2017/002737].

ORCID

Ajay D. Jagadale https://orcid.org/0000-0003-2694-0757
R. C. Rohit https://orcid.org/0000-0002-6601-1891

References

1. B. Wang, T. Ruan, Y. Chen, F. Jin, L. Peng, Y. Zhou, D. Wang, and S. Dou, *Energy Storage Mater.*, **24**, 22 (2020).
2. D. Chen, K. Jiang, T. Huang, and G. Shen, *Adv. Mater.*, **32**, 1901806 (2020).
3. P. Simon and Y. Gogotsi, *Nat. Mater.*, **19**, 1151 (2020).
4. A. Jagadale, X. Zhou, R. Xiong, D. P. Dubal, and J. Xu, S, *Energy Storage Mater.*, **19**, 314 (2019).
5. S. Chen, L. Qiu, and H.-M. Cheng, *Chem. Rev.*, **120**, 2811 (2020).
6. J. Yin, W. Zhang, N. A. Alhebshi, N. Salah, and H. N. Alshareef, *Small Methods*, **4**, 1900853 (2020).
7. G. Wang, L. Zhang, and J. Zhang, *Chem. Soc. Rev.*, **41**, 797 (2012).
8. V. Augustyn, P. Simon, and B. Dunn, *Energy Environ. Sci.*, **7**, 1597 (2014).
9. C. Liu, Z. Yu, D. Neff, A. Zhamu, and B. Z. Jang, *Nano Lett.*, **10**, 4863 (2010).
10. L. M. Da Silva, R. Cesar, C. M. R. Moreira, J. H. M. Santos, L. G. De Souza, B. M. Pires, R. Vicentini, W. Nunes, and H. Zanin, *Energy Storage Mater.*, **27**, 555 (2020).
11. S. Zhai, L. Wei, H. E. Karahan, X. Chen, C. Wang, X. Zhang, J. Chen, X. Wang, and Y. Chen, *Energy Storage Mater.*, **19**, 102 (2019).
12. J. Liu, J. Wang, C. Xu, H. Jiang, C. Li, L. Zhang, J. Lin, and Z. X. Shen, *Adv. Sci.*, **5**, 1700322 (2018).
13. I. S. Ike, I. Sigalas, and S. Iyuke, *Phys. Chem. Chem. Phys.*, **18**, 661 (2015).
14. S. A. Kazaryan, G. G. Kharisov, S. V. Litvinenko, and V. I. Kogan, *J. Electrochem. Soc.*, **154**, A751 (2007).
15. Z. Wang et al., *J. Mater. Chem. A*, **7**, 8633 (2019).
16. M. Xia, J. Nie, Z. Zhang, X. Lu, and Z. L. Wang, *Nano Energy*, **47**, 43 (2018).
17. L. Jamieson, T. Roy, and H. Wang, *J. Energy Storage*, **33**, 102075 (2021).
18. Y. Zhang and H. Yang, *J. Power Sources*, **196**, 4128 (2011).
19. H. Yang and Y. Zhang, *J. Power Sources*, **196**, 8866 (2011).
20. J. W. Graydon, M. Panjehshahi, and D. W. Kirk, *J. Power Sources*, **245**, 822 (2014).
21. A. D. Pasquier, A. Laforgue, P. Simon, G. G. Amatucci, and J.-F. Fauvarque, *J. Electrochem. Soc.*, **149**, A302 (2002).
22. X. Fan, Y. Li, S. Wang, Y. Lu, H. Xu, J. Liu, and C. Yan, *Electrochim. Acta*, **176**, 70 (2015).
23. T. Nguyen and M. F. Montemor, *J. Mater. Chem. A*, **6**, 2612 (2018).
24. H. A. Andreas, *J. Electrochem. Soc.*, **162**, A5047 (2015).
25. K. Liu, C. Yu, W. Guo, L. Ni, J. Yu, Y. Xie, Z. Wang, Y. Ren, and J. Qiu, *J. Energy Chem.*, **58**, 94 (2021).
26. Q. Zhang, J. Rong, D. Ma, and B. Wei, *Energy Environ. Sci.*, **4**, 2152 (2011).
27. B. E. Conway, W. G. Pell, and T.-C. Liu, *J. Power Sources*, **65**, 53 (1997).
28. J. Niu, W. G. Pell, and B. E. Conway, *J. Power Sources*, **156**, 725 (2006).
29. S. A. Kazaryan, S. V. Litvinenko, and G. G. Kharisov, *J. Electrochem. Soc.*, **155**, A464 (2008).
30. J. Kowal, E. Avaroglu, F. Chamekh, A. Šenfelds, T. Thien, D. Wijaya, and D. U. Sauer, *J. Power Sources*, **196**, 573 (2011).
31. C. Hao, X. Wang, Y. Yin, and Z. You, *J. Electron. Mater.*, **45**, 2160 (2016).
32. O. Okhay, A. Tkach, P. Staiti, and F. Lufrano, *Electrochim. Acta*, **353**, 136540 (2020).
33. W. Zhang, W. Yang, H. Zhou, Z. Zhang, M. Zhao, Q. Liu, J. Yang, and X. Lu, *Electrochim. Acta*, **357**, 136855 (2020).
34. J. Hansson, Q. Li, A. Smith, I. Zakaria, T. Nilsson, A. Nylander, L. Ye, P. Lundgren, J. Liu, and P. Enoksson, *J. Power Sources*, **451**, 227765 (2020).
35. M. Haque, Q. Li, C. Rigato, A. Rajaras, A. D. Smith, P. Lundgren, and P. Enoksson, *J. Power Sources*, **485**, 229328 (2021).
36. T. Tevi, H. Yaghoubi, J. Wang, and A. Takshi, *J. Power Sources*, **241**, 589 (2013).
37. T. Tevi and A. Takshi, *J. Power Sources*, **273**, 857 (2015).
38. T. Xiong, Z. G. Yu, W. S. V. Lee, and J. Xue, *ChemSusChem*, **11**, 3307 (2018).
39. S. Sun, D. Rao, T. Zhai, Q. Liu, H. Huang, B. Liu, H. Zhang, L. Xue, and H. Xia, *Adv. Mater.*, **32**, 2005344 (2020).
40. K. Wang, J. Wang, S. Zhao, Z. Wang, and S. Wang, *J. Power Sources*, **434**, 226745 (2019).
41. X. Zhang, X. Wang, J. Su, X. Wang, L. Jiang, H. Wu, and C. Wu, *J. Power Sources*, **199**, 402 (2012).
42. M. Haque, Q. Li, A. D. Smith, V. Kuzmenko, P. Rudquist, P. Lundgren, and P. Enoksson, *J. Power Sources*, **453**, 227897 (2020).
43. Z. Huang et al., *Angew. Chem. Int. Ed.*, **60**, 1011 (2021).
44. T. An and W. Cheng, *J. Mater. Chem. A*, **6**, 15478 (2018).
45. Q. Huang, D. Wang, and Z. Zheng, *Adv. Energy Mater.*, **6**, 1600783 (2016).
46. J. Zang, C. Cao, Y. Feng, J. Liu, and X. Zhao, *Sci. Rep.*, **4**, 6492 (2014).
47. Y. Xu, Z. Lin, X. Huang, Y. Wang, Y. Huang, and X. Duan, *Adv. Mater.*, **25**, 5779 (2013).
48. J.-Y. Luo, D.-D. Zhou, J.-L. Liu, and Y.-Y. Xia, *J. Electrochem. Soc.*, **155**, A789 (2008).
49. H. Li, T. Lv, N. Li, Y. Yao, K. Liu, and T. Chen, *Nanoscale*, **9**, 18474 (2017).
50. X. Gong, S. Li, and P. S. Lee, *Nanoscale*, **9**, 10794 (2017).
51. L.-Q. Fan, Q.-M. Tu, C.-L. Geng, Y.-L. Wang, S.-J. Sun, Y.-F. Huang, and J.-H. Wu, *Int. J. Hydrog. Energy*, **45**, 17131 (2020).
52. L.-Q. Fan, Q.-M. Tu, C.-L. Geng, J.-L. Huang, Y. Gu, J.-M. Lin, Y.-F. Huang, and J.-H. Wu, *Electrochim. Acta*, **331**, 135425 (2020).
53. M. Chen, G. Feng, and R. Qiao, *Curr. Opin. Colloid Interface Sci.*, **47**, 99 (2020).
54. H. Avireddy et al., *Nano Energy*, **64**, 103961 (2019).
55. X. Zhang, X. Wang, L. Jiang, H. Wu, C. Wu, and J. Su, *J. Power Sources*, **216**, 290 (2012).
56. Y. Luo, Q. Zhang, W. Hong, Z. Xiao, and H. Bai, *Phys. Chem. Chem. Phys.*, **20**, 131 (2018).
57. H. Wang, J. Chen, R. Fan, and Y. Wang, *Sustain. Energy Fuels*, **2**, 2727 (2018).
58. B. Wang, P. Guo, H. Bi, Q. Li, G. Zhang, R. Wang, J. Liu, and X. S. Zhao, *Int. J. Electrochem. Sci.*, **8**, 12 (2013).
59. K. Fic, G. Lota, and E. Frackowiak, *Electrochim. Acta*, **55**, 7484 (2010).
60. M. Tachibana, T. Ohishi, Y. Tsukada, A. Kitajima, H. Yamagishi, and M. Murakami, *Electrochemistry*, **79**, 882 (2011).
61. H. Peng, L. Xiao, K. Sun, G. Ma, G. Wei, and Z. Lei, *J. Power Sources*, **435**, 226800 (2019).
62. K. Wang, L. Yao, M. Jahon, J. Liu, M. Gonzalez, P. Liu, V. Leung, X. Zhang, and T. N. Ng, *ACS Energy Lett.*, **5**, 3276 (2020).
63. J. Lee, S. Choudhury, D. Weingarth, D. Kim, and V. Presser, *ACS Appl. Mater. Interfaces*, **8**, 23676 (2016).
64. X.-Z. Sun, X. Zhang, B. Huang, and Y.-W. Ma, *Acta Phys.-Chim. Sin.*, **30**, 485 (2014).
65. Z. Huang et al., *Adv. Energy Mater.*, **10**, 2001024 (2020).
66. Y. Wang, X. Qiao, C. Zhang, and X. Zhou, *Energy*, **159**, 1035 (2018).
67. A. Du Pasquier, I. Plitz, S. Menocal, and G. Amatucci, *J. Power Sources*, **115**, 171 (2003).
68. H. Talbi, P.-E. Just, and L. H. Dao, *J. Appl. Electrochem.*, **33**, 465 (2003).
69. S.-L. Kuo and N.-L. Wu, *J. Power Sources*, **162**, 1437 (2006).
70. Y.-P. Lin and N.-L. Wu, *J. Power Sources*, **196**, 851 (2011).
71. F. Yu, M. Huang, J. Wu, Z. Qiu, L. Fan, J. Lin, and Y. Lin, *J. Appl. Polym. Sci.*, **131**, 39784 (2014).
72. L. Cheng, P. Guo, R. Wang, L. Ming, F. Leng, H. Li, and X. S. Zhao, *Colloids Surf. Physicochem. Eng. Asp.*, **446**, 127 (2014).
73. C. Wu, X. Wang, Q. Zhao, J. Gao, Y. Bai, and H. Shu, *Trans. Nonferrous Met. Soc. China*, **24**, 3541 (2014).
74. R. Yi, S. Chen, J. Song, M. L. Gordin, A. Manivannan, and D. Wang, *Adv. Funct. Mater.*, **24**, 7433 (2014).
75. L. Chen, Y. Chen, J. Wu, J. Wang, H. Bai, and L. Li, *J. Mater. Chem. A*, **2**, 10526 (2014).
76. N. Li, J. Xu, H. Chen, and X. Wang, *J. Nanosci. Nanotechnol.*, **14**, 5157 (2014).
77. A. S. Pillai, R. Rajagopalan, A. Amruthalakshmi, J. Joseph, A. Ajay, I. Shakir, S. V. Nair, and A. Balakrishnan, *Colloids Surf. Physicochem. Eng. Asp.*, **470**, 280 (2015).
78. J. Wang, B. Ding, X. Hao, Y. Xu, Y. Wang, L. Shen, H. Dou, and X. Zhang, *Carbon*, **102**, 255 (2016).
79. C. Yang, L. Zhang, N. Hu, Z. Yang, H. Wei, Z. J. Xu, Y. Wang, and Y. Zhang, *Appl. Surf. Sci.*, **379**, 206 (2016).
80. C. Yang, L. Zhang, N. Hu, Z. Yang, H. Wei, Y. Wang, and Y. Zhang, *Appl. Surf. Sci.*, **387**, 666 (2016).
81. C. Yang, L. Zhang, N. Hu, Z. Yang, H. Wei, and Y. Zhang, *J. Power Sources*, **302**, 39 (2016).
82. X.-L. Dong, A.-H. Lu, B. He, and W.-C. Li, *J. Power Sources*, **327**, 535 (2016).
83. F. Miao, C. Shao, X. Li, N. Lu, K. Wang, X. Zhang, and Y. Liu, *Energy*, **95**, 233 (2016).
84. G. P. Pandey, S. A. Klankowski, T. Liu, J. Wu, and J. Li, *J. Power Sources*, **342**, 1006 (2017).
85. B. Song et al., *Nano Energy*, **31**, 183 (2017).
86. F. N. Ajjan, M. Vagin, T. Rębiś, L. E. Aguirre, L. Ouyang, and O. Inganäs, *Adv. Sustain. Syst.*, **1**, 1700054 (2017).
87. B. Saravanakumar, S. Sivabalan Jayaseelan, M.-K. Seo, H.-Y. Kim, and B.-S. Kim, *Nanoscale*, **9**, 18819 (2017).
88. D. Momodu, A. Bello, K. Oyedotun, F. Ochai-Ejeh, J. Dangbegnon, M. Madito, and N. Manyala, *RSC Adv.*, **7**, 37286 (2017).
89. S. Wang, X. Wang, Z. Bao, X. Yang, L. Ye, and L. Zhao, *J. Mater. Chem. A*, **5**, 10227 (2017).
90. D. Liu, C. Fu, N. Zhang, Y. Li, H. Zhou, and Y. Kuang, *J. Solid State Electrochem.*, **21**, 759 (2017).
91. W. Quan, C. Jiang, S. Wang, Y. Li, Z. Zhang, Z. Tang, and F. Favier, *Electrochim. Acta*, **247**, 1072 (2017).
92. K. Li, J. Liu, Y. Huang, F. Bu, and Y. Xu, *J. Mater. Chem. A*, **5**, 5466 (2017).
93. A. J. Paleo, P. Staiti, A. Brigandì, F. N. Ferreira, A. M. Rocha, and F. Lufrano, *Energy Storage Mater.*, **12**, 204 (2018).
94. S. Deshagani, K. Krushnamurty, and M. Deepa, *Mater. Today Energy*, **9**, 137 (2018).
95. A. Das, S. Deshagani, R. Kumar, and M. Deepa, *ACS Appl. Mater. Interfaces*, **10**, 35932 (2018).
96. H. Gao, X. Wang, G. Wang, C. Hao, S. Zhou, and C. Huang, *Nanoscale*, **10**, 10190 (2018).
97. S.-E. Chun, S. J. Yoo, and S. W. Boettcher, *J. Electrochem. Sci. Technol.*, **9**, 20 (2018).
98. Z. Gao, C. Chen, J. Chang, L. Chen, P. Wang, D. Wu, F. Xu, and K. Jiang, *Chem. Eng. J.*, **343**, 572 (2018).
99. B. Moyo, D. Momodu, O. Fasakin, A. Bello, J. Dangbegnon, and N. Manyala, *J. Mater. Sci.*, **53**, 5229 (2018).
100. R. K. Mishra, M. Krishnaih, S. Y. Kim, A. K. Kushwaha, and S. H. Jin, *Mater. Lett.*, **236**, 167 (2019).
101. R. K. Mishra, G. J. Choi, Y. Sohn, S. H. Lee, and J. S. Gwag, *Mater. Lett.*, **245**, 192 (2019).
102. I. Aldama, K. I. Siwek, J. M. Amarilla, J. M. Rojo, S. Eugénio, T. M. Silva, and M. F. Montemor, *J. Energy Storage*, **22**, 345 (2019).
103. Y. He, X. Wang, H. Huang, P. Zhang, B. Chen, and Z. Guo, *Appl. Surf. Sci.*, **469**, 446 (2019).
104. D. Qu, X. You, X. Feng, J. Wu, D. Liu, D. Zheng, Z. Xie, D. Qu, J. Li, and H. Tang, *Appl. Surf. Sci.*, **463**, 879 (2019).

105. Z. Gao, L. Chen, J. Chang, Z. Wang, D. Wu, F. Xu, and K. Jiang, *Int. J. Hydrog. Energy*, **44**, 10554 (2019).
106. M. Abdollahifar, S.-S. Huang, Y.-H. Lin, H.-S. Sheu, J.-F. Lee, M.-L. Lu, Y.-F. Liao, and N.-L. Wu, *J. Power Sources*, **412**, 545 (2019).
107. N. Zhao, H. Fan, J. Ma, M. Zhang, C. Wang, H. Li, X. Jiang, and X. Cao, *J. Power Sources*, **439**, 227097 (2019).
108. C. Xiao, W. Zhang, H. Lin, Y. Tian, X. Li, Y. Tian, and H. Lu, *New Carbon Mater.*, **34**, 341.
109. Y. Lu, Z. Li, Z. Bai, H. Mi, C. Ji, H. Pang, C. Yu, and J. Qiu, *Nano Energy*, **66**, 104132 (2019).
110. Z. Li, S. He, C. Ji, H. Mi, C. Lei, Z. Li, H. Pang, Z. Fan, C. Yu, and J. Qiu, *Adv. Mater. Interfaces*, **6**, 1900959 (2019).
111. H. Shao, N. Padmanathan, D. McNulty, C. O'Dwyer, and K. M. Razeeb, *ACS Appl. Energy Mater.*, **2**, 569 (2019).
112. X. Wang, Y. He, Z. Guo, H. Huang, P. Zhang, and H. Lin, *New J. Chem.*, **43**, 18813 (2019).
113. C.-L. Geng, L.-Q. Fan, C.-Y. Wang, Y.-L. Wang, S.-J. Sun, Z.-Y. Song, N. Liu, and J.-H. Wu, *New J. Chem.*, **43**, 18935 (2019).
114. T. Liang, H. Wang, R. Fei, R. Wang, B. He, Y. Gong, and C. Yan, *Nanoscale*, **11**, 20715 (2019).
115. B. Jinisha, K. M. Anilkumar, M. Manoj, C. M. Ashraf, V. S. Pradeep, and S. Jayalekshmi, *J. Solid State Electrochem.*, **23**, 3343 (2019).
116. A. Khazaeli, G. Godbille-Cardona, and D. P. J. Barz, *Adv. Funct. Mater.*, **30**, 1910738 (2020).
117. K. Lota, I. Acznik, A. Sierczynska, and G. Lota, *J. Appl. Polym. Sci.*, **137**, 48867 (2020).
118. Y. Yuan, Y. Lu, B. Jia, H. Tang, L. Chen, Y. Zeng, Y. Hou, Q. Zhang, Q. He, L. Jiao, J. Leng, Z. Ye, and J. Lu, *Nano-Micro Lett.*, **11**, 42 (2019).
119. M. M. Ovhal, N. Kumar, S.-K. Hong, H.-W. Lee, and J.-W. Kang, *J. Alloys Compd.*, **828**, 154447 (2020).
120. S. Dsoke and Q. Abbas, *ChemElectroChem*, **7**, 2466 (2020).
121. G. Zhang, T. Guan, N. Wang, J. Wu, J. Wang, J. Qiao, and K. Li, *Chem. Eng. J.*, **399**, 125818 (2020).
122. V. C. Wakchaure, A. R. Kottaichamy, A. D. Nidhankar, K. C. Ranjeesh, M. A. Nazrulla, M. O. Thotiyl, and S. S. Babu, *ACS Appl. Energy Mater.*, **3**, 6352 (2020).
123. G. Nikiforidis, S. Wustoni, D. Ohayon, V. Druet, and S. Inal, *ACS Appl. Energy Mater.*, **3**, 7896 (2020).
124. S. Deshagani, A. Das, D. Nepak, and M. Deepa, *ACS Appl. Polym. Mater.*, **2**, 1190 (2020).
125. B. B. Beenarani and C. P. Sugumaran, *Ionics*, **26**, 1465 (2020).
126. J. Chang, S. Zang, Y. Wang, C. Chen, D. Wu, F. Xu, K. Jiang, Z. Bai, and Z. Gao, *Electrochim. Acta*, **353**, 136501 (2020).
127. R. Kumar Mishra, G. Jin Choi, Y. Sohn, and S. Hee Lee, *J. Seog Gwag, Chem. Commun.*, **56**, 2893 (2020).
128. L.-Q. Fan, C.-L. Geng, Y.-L. Wang, S.-J. Sun, Y.-F. Huang, and J.-H. Wu, *New J. Chem.*, **44**, 17070 (2020).
129. X. Ma, J. Wang, X. Wang, L. Zhao, and C. Xu, *J. Mater. Sci., Mater. Electron.*, **30**, 5478 (2019).
130. S. Yuan, X. Huang, H. Wang, L. Xie, J. Cheng, Q. Kong, G. Sun, and C.-M. Chen, *J. Energy Chem.*, **51**, 396 (2020).
131. C. Poochai, C. Sriprachuabwong, J. Sodtipinta, J. Lohitkarn, P. Pasakon, V. Primpray, N. Maeboonruan, T. Lomas, A. Wisitsoraat, and A. Tuantranont, *J. Colloid Interface Sci.*, **583**, 734 (2021).
132. K. Song, R. Yang, X. Chen, X. Wang, G. Chen, and N. Zhao, *Appl. Surf. Sci.*, **542**, 148670 (2021).
133. R. K. Mishra, D. Mishra, M. Krishnaiah, S. Y. Kim, and S. H. Jin, *Ceram. Int.*, **47**, 11231 (2021).
134. Y. Li, W. Yang, W. Yang, Z. Wang, J. Rong, G. Wang, C. Xu, F. Kang, and L. Dong, *Nano-Micro Lett.*, **13**, 95 (2021).